ISMRM 2024 – Engineering Study Group Challenge

Team name:

MoPHA Vienna

Names, email addresses, and affiliations of members:

Ernesto Gomez Tamm[1] (e.gomez.tamm@gmail.com)
Jean-Lynce Gnanago[1] (jean-lynce.gnanago@meduniwien.ac.at)
Andreas Hodul[2] (andreas.hodul@meduniwien.ac.at)
Markus Ortner[3] (markus.ortner@meduniwien.ac.at)
Quang Nguyen[2] (quang.nguyen@meduniwien.ac.at)
Onisim Soanca[1] (onisim.soanca@meduniwien.ac.at)
Zacharias Chalampalakis[3] (zacharias.chalampalakis@meduniwien.ac.at)
Ivo Rausch[3] (ivo.rausch@meduniwien.ac.at)
Elmar Laistler[1] (elmar.laistler@meduniwien.ac.at)
Roberta Frass-Kriegl[1] (roberta.frass@meduniwien.ac.at)

[1]High-field MR Center, Center for Medical Physics and Biomedical Engineering, Medical University of Vienna, Vienna, Austria

[2]Center for Medical Physics and Biomedical Engineering, Medical University of Vienna, Vienna, Austria

[3]QIMP Team, Center for Medical Physics and Biomedical Engineering, Medical University of Vienna, Vienna, Austria

Link to repository:

https://zenodo.org/records/10997616

doi: 10.5281/zenodo.10997616

Description of how the tool can be used to advance MRI research (max. 500 words):

For magnetic resonance imaging (MRI) of the torso, motion presents a challenge due to inevitable respiratory and cardiac motion. Depending on the image acquisition technique, motion can cause artifacts, including blurring, ghosting, signal dropouts and unwanted signal enhancement. Therefore, motion tracking and compensation are subject of past and ongoing research. The development of such techniques requires suitable phantoms that provide user-defined motion models with sufficient

spatial/temporal accuracy and reproducibility. This project presents a dynamic torso motion phantom that can serve as ground truth for the investigation and characterization of motion compensation and tracking methods.

The phantom has three degrees of freedom (DOFs): (1) breathing motion of the chest wall predominately in anteroposterior direction (10 mm max. amplitude, 0.5 Hz max. rate), (2) breathing motion of the heart and the abdominal organs in craniocaudal direction (45 mm max. amplitude, 0.5 Hz max. rate), (3) simplified cardiac motion in craniocaudal direction (19 mm amplitude, 3 Hz max. rate). The primary target application is the characterization and validation of novel motion tracking methods. Therefore, mechanical motion models, i.e. simple moving objects, are prioritized over functional and physiological features like blood flow, for instance. Expected benefits in comparison to other torso phantoms featuring both, breathing and cardiac motion, are higher accuracy thanks to used actuators and the possibility of clearly separating cardiac, chest and diaphragm motion.

What is included in the open source repository?

- Complete CAD model of the developed phantom
- List of all parts used/required for construction
- Some illustrations
- MATLAB script to control the heart module of the phantom

What is not included in the open source repository?

- Control software for the breathing modules (This was done via the user interface provided by the vendor of the respective actuators).

The phantom is mostly constructed from low-cost components with standard plastic processing techniques (milling, 3D printing). Exceptions are the custom-made outer shell and the breathing actuators, both of which were very expensive. To save costs, these components could be replaced by a rectangular box and 3D printed pneumatic stepper motors (reduced accuracy and speed), respectively.

Description of the tool's functionality and capabilities (1000 words + 4 figs):

Disclaimer – The attached detailed description is a merge of an ISMRM abstract (Gomez Tamm et al., no. 1319, 2024) and an ESMRMB abstract submitted in May 2024 (Gnanago et al.).

Modular Torso Motion Phantom for MRI

Ernesto Gomez Tamm[1], Jean-Lynce Gnanago[1], Andreas Hodul[2], Markus Ortner[3], Quang Nguyen[2], Onisim Soanca[1], Zacharias Chalampalakis[3], Ivo Rausch[3], Elmar Laistler[1], Roberta Frass-Kriegl[1]

[1]High-field MR Center, Center for Medical Physics and Biomedical Engineering, Medical University of Vienna, Vienna, Austria
[2]Center for Medical Physics and Biomedical Engineering, Medical University of Vienna, Vienna, Austria
[3]QIMP Team, Center for Medical Physics and Biomedical Engineering, Medical University of Vienna, Vienna, Austria

Motivation

For magnetic resonance imaging (MRI) of the torso, motion presents a challenge due to inevitable respiratory and cardiac motion. Depending on the image acquisition technique, motion can cause artifacts, including blurring, ghosting, signal dropouts and unwanted signal enhancement. Therefore, motion tracking and compensation are subject of past and ongoing research. This project presents a dynamic torso motion phantom with sufficient spatial/temporal accuracy and repeatability to serve as ground truth for the investigation of novel motion tracking methods.

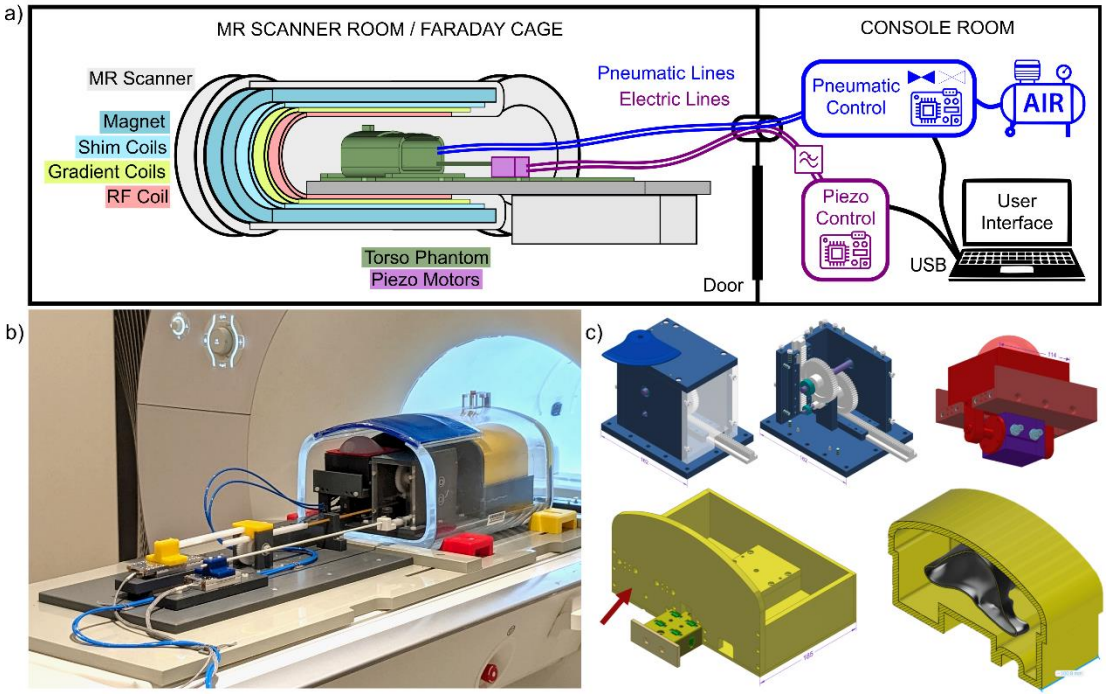

Figure 1. Phantom construction. *a) Set-up of the phantom and the control unit in the MRI environment. b) Photograph of the phantom at the opening of the 3 T MRI bore. c) Detailed isometric CAD drawings of the motion modules. Blue: Gear box for chest motion. Yellow: Monorail track and wagon for abdominal organ motion (left) and a sectional view of the bulk shell and the liver phantom (right). The position at which the heart module is attached to the wagon is indicated by the red arrow. Red: Heart module with sliding box, heart phantom and double-action pneumatic cylinder.*

Phantom development

Figure 1 shows the dynamic torso phantom with its motion modules featuring three degrees of freedom (DOFs): (1) breathing motion of the chest wall in anteroposterior direction (10 mm max. amplitude, 0.5 Hz max. rate), (2) breathing motion of the heart and the abdominal organs in craniocaudal direction (45 mm max. amplitude, 0.5 Hz max. rate), (3) simplified cardiac motion in craniocaudal direction (19 mm amplitude, 3 Hz max. rate).

The motion modules are enclosed in a double-walled acrylic shell filled with saline solution (approx. 5 L deionized water, 5 g/L NaCl, 1 ml/L Gadoteriol contrast agent). The top front part of the shell is not covered by acrylic glass but by a low-cost commercially available gel mat (290 x 290 x 10 mm, polyurethane) representing the chest wall. Breathing motion (DOF 1 & 2) is realized with two independently controlled non-magnetic linear piezo stages (Xeryon, Belgium) with 3 N nominal driving force, 109 mm maximum travel range, speeds of up to 200 mm/s and spatial accuracy in the µm range.

For chest motion (DOF 1), the horizontal movement of the piezo stage is translated into a vertical movement via a gear box (Fig. 1c) containing a compound gear with a ratio of 1:5, providing an increase of the driving force. For abdominal organ motion (DOF 2), a monorail track and a bulk shell on a wagon were constructed (Fig.1c). In the bulk shell, different organ phantoms can be placed (e.g., the additively manufactured liver mock-up shown in Fig.1c). The heart module is attached to the abdominal organ wagon to emulate heart movement with breathing. A gear box with a ratio of 1:2 connects the wagon to the respective piezo stage.

To mimic heartbeat motion (DOF 3), a sliding box holding a heart phantom (i.e., SLA-printed heart segmented from an MRI scan filled with approximately 300 g gel made of 48.34 % (weight percent) deionized water, 48.34 % ethylene glycol, 0.58 % NaCl, 1.93 % Agarose, 0.39 % KH_2PO_4, 0.34 % K_2HPO_4, 0.05 % Sodium azide, and 0.02 % Magnetvist contrast agent), and a full-plastic pneumatic movement system connected underneath were designed (Fig. 1c). The phosphorous components were added to facilitate ^{31}P MR spectroscopy experiments in the future. A double-action piston is used to avoid the need for a metal spring for retraction. The pneumatic system is supplied with compressed air (1.5 bar) from outside the scanner room via electromagnetic valves (Festo GmbH, Germany) actuated by a MATLAB-controlled data acquisition card (NI-USB-6001, National Instruments, USA), Fig.1a.

Characterization of motion capabilities

First MR data (2D FLASH, T_R = 7.5 ms, T_E = 3.69 ms, slice thickness 7 mm, FOV 350 x 350 mm^2, acq. matrix 256 x 233, 2 averages, *TA* = 6 x 3.48 s)) were acquired without motion resulting in artifact-free images, Fig.2a.

To characterize and validate the motion capabilities of the phantom, four human-inspired motion patterns are defined, Fig. 2b. An illustration of motion artifacts caused by each investigated pattern are shown in Fig.2c. Here, linear breathing patterns achieved by driving the stages back and forth at constant speed are used. However, the piezo stages are capable of arbitrary user defined motion patterns.

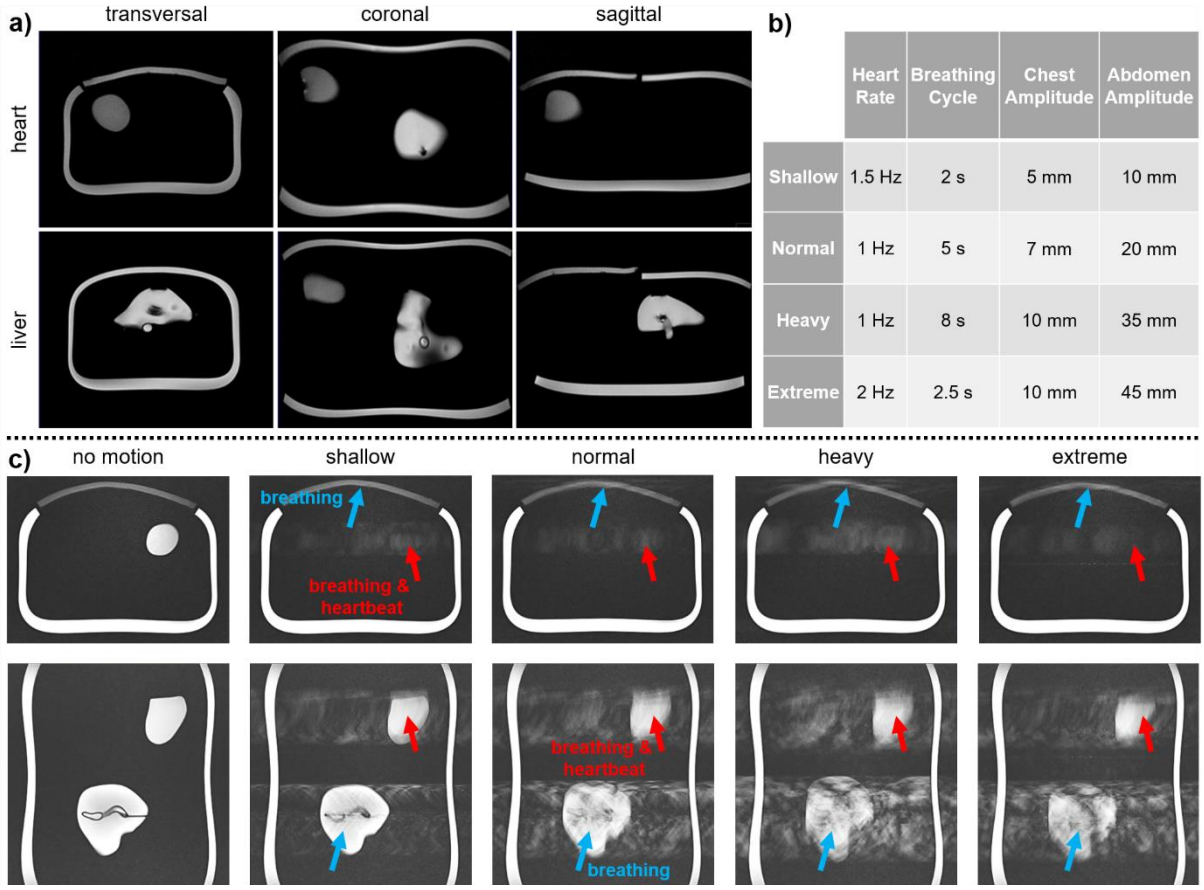

	Heart Rate	Breathing Cycle	Chest Amplitude	Abdomen Amplitude
Shallow	1.5 Hz	2 s	5 mm	10 mm
Normal	1 Hz	5 s	7 mm	20 mm
Heavy	1 Hz	8 s	10 mm	35 mm
Extreme	2 Hz	2.5 s	10 mm	45 mm

Figure 2. MR images and motion patterns. *a) 2D FLASH images of the static phantom. Slices are centered at the heart phantom (top row) and the liver phantom (bottom row), respectively. Apart from image distortions at the edges of the large FOV (450 mm in z-direction) due to typical gradient nonlinearities, no imaging artifacts are observable. b) Defined motion patterns. c) Axial and coronal T_2-weighted MR images (TR = 1980 ms, TE = 65 ms, FOV = 280 mm x 368 mm, 12 slices, voxel size 0.9 mm x 0.9 mm x 3 mm, phase encoding: R >> L) of the moving phantom and respective motion artifact.*

To demonstrate that the motion performance of the piezo stages is not impaired by the MR environment, we recorded time courses of all four motion scenarios outside and inside the MR scanner (3T Prisma Fit, Siemens, Germany) while running one T_1-weighted (axial; TR = 3.7 ms, TE = 1.13 ms, FOV = 280 x 368 mm^2, 256 slices, voxel size 1.5 x 1.5 x 1 mm^3) and two T_2-weighted (axial and coronal; TR = 1980 ms, TE = 65 ms, FOV = 280 x 368 mm^2, 12 slices, voxel size 0.9 x 0.9 x 3 mm^3) sequences that approached the limits of gradient induced peripheral nerve stimulation and RF induced specific absorption rate, respectively (approx. 5 min in total). Further, to investigate the general repeatability of the phantom performance, the outside-scanner measurement was repeated after one week (incl. setting-up controllers and tracking system). Time series of breathing motions are recorded using the internal position logging function of the piezo stage controller. Frequency and amplitude values are extracted from the time series of different measurement sessions. The phantom's breathing motion performance is presented in Fig.3.

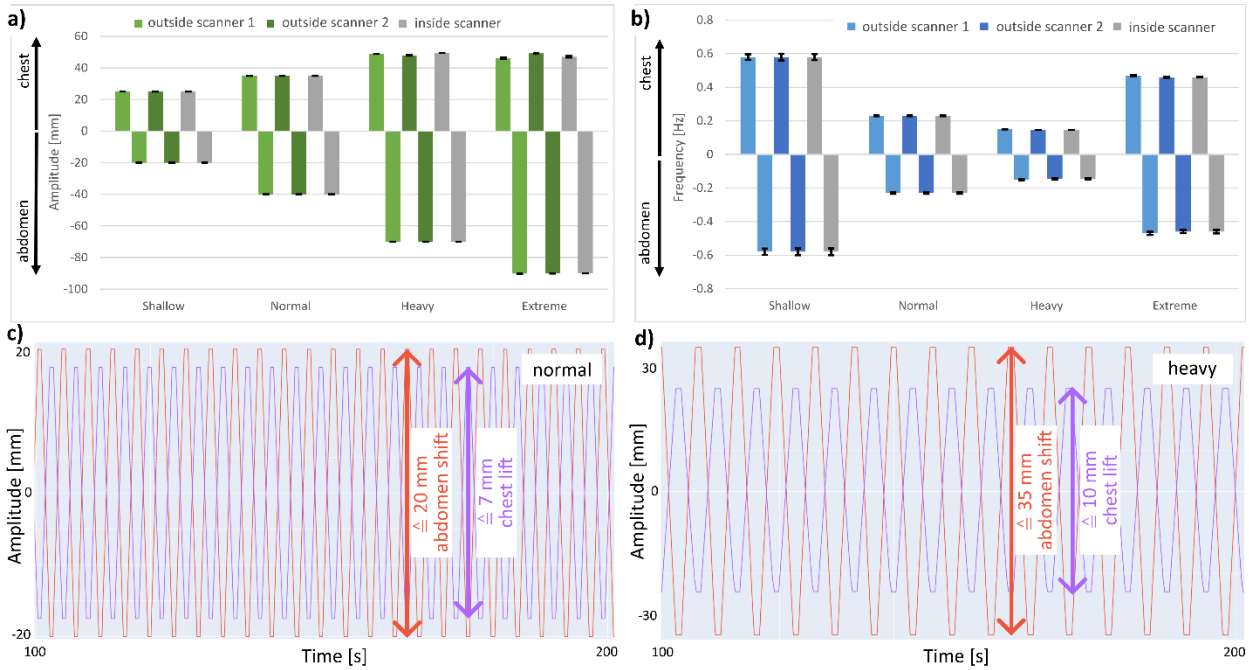

Figure 3. Breathing motion. *a) Maximum displacement amplitude of the piezo stages for the investigated motion patterns. b) Displacement frequency of the piezo stages. Error bars in a)+b) represent standard deviations. c)+d) Exemplary section of the piezo stage displacement time series for "normal" and "heavy" motion patterns.*

To characterize the motion of the heart module, an MR-adapted optical navigation system (Polaris VEGA, NDI, Waterloo, Canada) with two trackers is used. One tracker is placed on the heart module while the other is fixed in the field of view of the camera. By computing the relative displacement between the two trackers, we obtain the time series (20 Hz sample rate) of the heart motion to monitor its performances at different rates; results are presented in Fig.4.

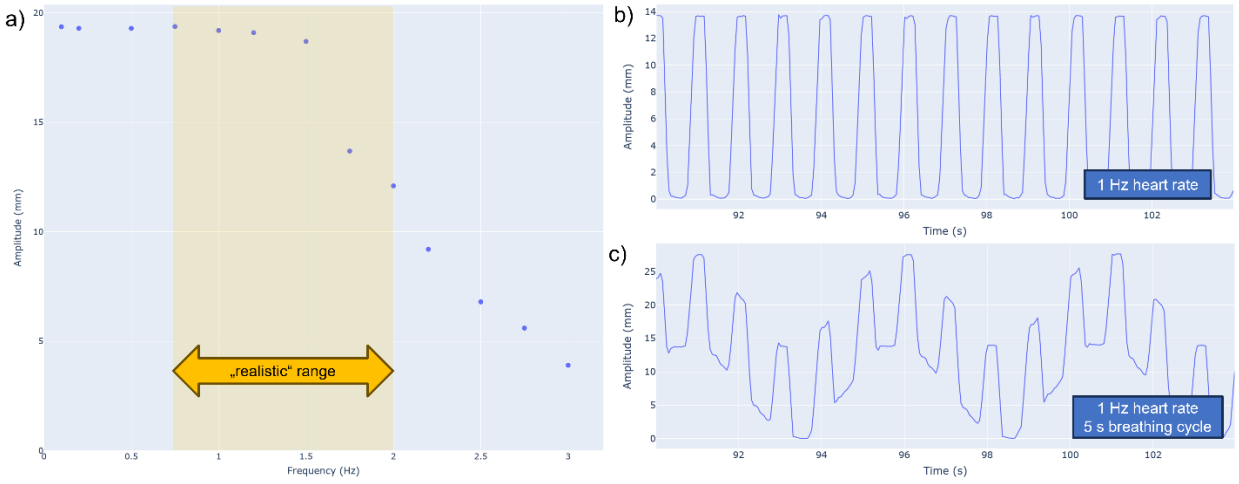

Figure 4. Heart motion. *a) Maximum amplitude of the heart motion at different heart rates. b) Example time series of the displacement of the heart module alone. c) Example time series of the displacement of the heart module combined with the breathing modules during the "normal" pattern.*

Discussion

Both, breathing frequency and amplitude are highly stable across the measurement series, indicating excellent repeatability of the motion patterns and robustness to the MR environment. For the heart module, high frequency stability was observed, however the amplitude decreased with heart rate above 1.5 Hz. This behavior was expected and is related to the design and construction of the full-plastic pneumatic cylinder, potential future modifications include improving the airtightness of the cylinder or reducing the motion range. Finally, the MR acquisitions showcase the motion artifacts induced by the different patterns, qualitatively showing that the severity of artifacts increases with motion intensity. The phantom can be used with different vendor whole-body scanners.

Acknowledgements

Austrian Science Fund (FWF) P37189-N and P35305-B, Focus Grants “T4MR” and “NoLimit” from CMPBME, MedUni Vienna.

Open source repository: https://zenodo.org/records/10997616